International Journal of Mechatronics and Applied Mechanics
2026, Issue 25, Vol. II

STUDY OF THE MARINE GAS TURBINE IMPELLER FORCED VIBRATION AND STRESS-STRAIN STATE

Natalia Smetankina [0000-0001-9528-3741], *Serhii Morhun* [0000-0003-2881-7541]
Anatolii Pidhornyi Institute of Power Machines and Systems, Kharkiv, Ukraine
Admiral Makarov National University of Shipbuilding, Mykolaiv, Ukraine
Email: nsmet@ipmach.kharkov.ua (✉), serhii.morhun@nuos.edu.ua

Abstract – The method of the marine gas turbine non-cooled impeller with damping links vibration research is described. Using the finite element method, a refined mathematical model was developed for the impeller's section, consisting of a disk sector and a blade with damping links. The developed mathematical model takes into consideration the structural heterogeneity of the blade itself and the disk. Also, the model takes into account the complex influence of mechanical and temperature contact interaction between rotor parts on the level of dynamic stresses in it. The proposed mathematical model differs from existing ones in using the Lagrange variational principle to take into account the contact interaction between parts of the blade crown, linking the potential energy of deformation during the contact interaction of solid bodies with the work of external forces in the contact zone. The results of the impeller forced vibration frequencies calculation, caused by the influence of non-stationary gas flow are given for the three most dangerous vibration modes. Also, for these vibration modes is given the stress-strain state. Obtained results can be used for further investigations, taking into account the problems of the impeller fatigue strength and fracture mechanics, that are especially important for the highly loaded marine gas turbine engines.

Keywords: Gas turbine, Impeller, Forced vibration, Stress-strain state, Vibration modes and frequencies.

1. Introduction

The task of the marine vehicles gas turbine engines (GTE) service life increasing is of practical interest and is an urgent problem in engineering. The rapid pace of turbine engines development is accompanied by a constant increase in the intensity of the processes occurring in them with a general increase in the requirements for their strength and reliability. Therefore, one of the basic tasks for the turbine impeller development is to calculate its vibration modes and frequencies together with its stress-strain state. The matter is that the blades are one of the most crucial elements of a turbine due to extremely hard-working conditions and their constructional heterogeneity, caused by a system of cooling channels in their cavities. So, one of the most important moments of the marine gas turbine engine design is not only the detuning of the impeller's natural frequencies and modes, but also a more comprehensive study of vibration processes in it, caused by an influence of a non-stationary gas flow.

Such research is also impossible without taking into consideration the processes of internal and structural damping in the blades feather joints, that are called "damping links". For all its complexity described problem requires the constant expansion and deepening of theoretical ideas about the dynamic phenomena associated with the working process of gas turbine engine.

Due to the high cost of modern turbines and especially works on their fine-tuning, the methods of their impeller's vibration characteristics determining are of great importance even at the design stage. Therefore, a comprehensive study of the vibration of the blade apparatus, taking into account the specifics of its elements and their interaction, is a serious scientific and practical problem, and, despite intensive research in this area [1–3], remains a number of unresolved aspects.

Thus, the use of simplified design schemes based on the application of the core theory [1] does not allow to identify the important features of the system, such as the influence of damping on the impeller's vibration frequencies. Within the

dx.doi.org/10.17683/ijomam/issue25/v2.26

framework of this theory, the blades are considered as twisted, inextensible and rigidly fixed in the disk rods of variable cross-section, making common-mode oscillations in one of the main bending planes. In [4], forced vibrations of the turbine engine impellers are investigated using the method of initial parameters; however, it does not indicate a method for the intensity of the disturbed gas dynamic forces calculating. In [3], asymptotic methods of nonlinear dynamics are used to solve the differential equations of impeller's forced vibration, but the damping in the system is not taken into account. In works [2, 5 - 8], this problem is solved using the finite element method, but in [9] the damping is not taken into account, and in [10], when constructing a finite-element mathematical model of an impeller, finite elements like "tetrahedron" are used, which do not allow take into consideration the blade constructional heterogeneity. The technique of compressors and turbines working blades free vibration frequencies experimental study is given in [11, 12], however, the experimental data are less reliable, since in the course of the experiment there are always unavoidable systemic errors of the experimental setup itself and measuring equipment.

2. Purpose of the Study

The development of a set of measures for the gas turbine's reliability increase is not feasible without a detailed study of vibration processes occurring in such critical details as impellers, influenced by non-stationary gas-dynamic forces of high temperature. However, as follows from the above analysis of recent research on this topic, some important aspects remain insufficiently illuminated, therefore, it is necessary to develop a refined mathematical model of the impeller forced vibration. It is also necessary to take into consideration the significant constructional heterogeneity of the impellers cooled blades.

Therefore, the aim of this work is to develop a refined mathematical model of the marine gas turbine cooled impeller with damping links, based on the usage of finite elements method. Full description of the finite elements that are suitable for the impeller correct modelling is given in the works [13, 14].

3. Study

3.1 Impeller Forced Vibration Determination

The task of the gas turbine impeller forced vibration amplitudes and frequencies determining is given. It is also assumed that the considered system of solid bodies (impeller) has the properties of cyclic symmetry. So, it can be interpreted as a set of h subsystems (sections) with the same geometric, inertial and stiffness properties [7]. In this case, h determines the system's order of symmetry. So, a section of such impeller generally includes a disk sector and a blade set in it with parts of damper links (fig. 1). The section is located in the rectangular right $X\ Y\ Z$ coordinate system: X axis coincides with the axis of turbine rotor rotation, Z axis is directed along the impeller radius, and the Y axis is perpendicular to the Z axis.

The finite element model of an impeller blade was built on the basis of superparametric curvilinear finite elements. Each of them consisted of 20 nodes with 5 degrees of freedom in every node. The damper links, connecting the blades in a unity were modeled using a rod finite element. The disk model included 230 first-order hexagonal finite elements with 1254 degrees of freedom totally.

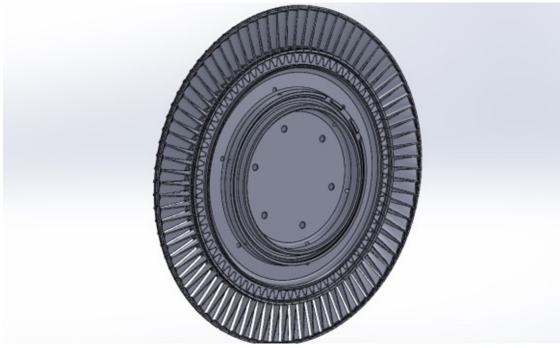

Figure 1: Impeller of the gas turbine engine

The value of pressure field, caused by the influence of non-stationary gas-dynamic flow is known. Due to the periodicity of the gas flow intensity, the function of pressure can be decomposed into a Fourier row:

$$p = p_1 \cos(k\omega t) + p_2 \sin(k\omega t) \quad (1)$$

(k=1,....,g)

where k is the number of the gas flow pressure harmonic; g is an amount of the harmonics; ω is the frequency of forced vibrations.

Taking into consideration (1) the equations of the section motion can be written as follows:

$$[M]\left\{\frac{d^2\delta}{dt^2}\right\} + [C]\left\{\frac{d\delta}{dt}\right\} + [K]\{\delta\} = \{p\} \quad (2)$$

where M is the mass matrix of the section; C is the matrix of damping; K s the stiffness matrix; δ is the generalized displacement vector of the section finite elements model; p is the vector of the gas flow pressure.

Let's do some transformations. Represent the generalized displacement vector {δ} as a decomposition into a Fourier row (3):

$$\delta_i = a_1 \cos(k\omega t) + a_2 \sin(k\omega t) \quad (3)$$

(i=1, 2,..., n)

where i is the number of the finite elements model nodes; n is a number of nodes.

Using the dependencies (1, 3), it is possible to transform the relation (2) for every finite element:

$$M_{ij}\left(a_1\cos(k\omega t)+a_2\sin(k\omega t)\right)^{//}+C_{ij}\left(a_1\cos(k\omega t)+a_2\sin(k\omega t)\right)^{/}+K_{ij}\left(a_1\cos(k\omega t)+a_2\sin(k\omega t)\right)=p_1\cos(k\omega t)+p_2\sin(k\omega t) \quad (4)$$

The system of equations (4) should be converted into the matrix equation (5), according to which the amplitudes of the impeller could be found.

$$\{S\}=\{a\}\{p\} \quad (5)$$

where S is the global matrix.

The set of forced vibration amplitudes for the impeller sections can be determined from the matrix equation (5). Consequently, the corresponding forced vibration frequencies can be calculated as follows:

$$[K]_{ij}a_i-\omega^2[M]_{ij}a_i=p_i \quad (6)$$

Equation (6) represents the so called generalized proper value problem. In general, its solution could be obtained as follows:

$$[A]x-\lambda[B]x=0 \quad (7)$$

where A and B are symmetric matrixes.

To solve matrix equation (7), Cholesky's positive definite decomposition algorithm [7] is applied. This yields to:

$$[B]=[L][M]\left[L^{-1}\right]^T \quad (8)$$
$$[A]=[K]=[L][L]^T$$

where L is the positive triangle matrix.

Thus, having solved the systems of matrix equations (5) and (6), it is possible to obtain the forced vibration amplitudes and frequencies of the impeller, excited by any harmonic of the gas flow.

3.2 Construction damping in the impeller

Considering the impeller, it is possible to assume that there is slippage between the contacting side surfaces of the adjacent blade's bandages. It is usually incomplete and is accompanied by dry friction processes on the surfaces of the bandages. It precisely depends on the magnitude of this slippage that the part of the kinetic energy of the blade vibrations will be spent on structural damping in the bandages.

When calculating, the installation tension on the bandages should be taken into account, which appears during the technological operations of impeller assembling. Therefore, to take it into account, it is appropriate to assume that "springs" of a given stiffness are installed between the bandages.

Internal damping in the impeller material is taken into account in a simplified way due to the lack of an established method for determining intermolecular bonds in the material and the discrepancy between its real crystal structure and the theoretical one due to the presence of impurity inclusions and the graininess of the material structure. Calculations of the impeller forced vibration amplitudes taking into account structural damping are carried out in the following sequence.

Determination of the exciting force, which leads to mutual displacements of the blade bandages.

For this case, the exciting force is the periodic gas-dynamic force $F(\varphi)$. It depends on the angle of rotation of the rotor φ and the pressure of the working fluid flow on the impeller. The force $F(\varphi)$ can be specified as an infinite sum of the terms of the trigonometric Fourier series.

$$F(\varphi)=F_0+F_1\cos(\varphi)+F_2\cos(2\varphi)+\ldots+F_k\cos(k\varphi)+P_1\sin(\varphi)+P_2\sin(2\varphi)+\ldots+P_k\sin(k\varphi) \quad (9)$$

$$F(\varphi)=F_0+\sum_{k=1}^{\infty}\left(F_k\cos(k\varphi)+P_k\sin(k\varphi)\right)$$

(φ = 0…360^0; k = 1…g)

where k is the harmonic number of the exciting force; F_0, F_k, P_k are the coefficients of the Fourier series

According to the theory of Fourier series, the coefficients of the series are defined as follows:

$$F_0=\frac{1}{2\pi}\int_0^{2\pi}F(\varphi)d\varphi$$
$$F_k=\frac{1}{\pi}\int_0^{2\pi}F(\varphi)\cos(k\varphi)d\varphi \quad (10)$$
$$P_k=\frac{1}{\pi}\int_0^{2\pi}F(\varphi)\sin(\varphi)d\varphi$$

(φ = 0…360^0; k = 1…g)

The constant term of the series F_0 is the average value of the static force, which causes the appearance of bending and torsional deformations. The second part of the series is a time-varying exciting force, consisting of an infinite number of harmonic forces with amplitudes F_k and P_k.

Considering the angular velocity of the rotor Ω as a constant, the angle of rotation of the rotor φ is equal to

$$\varphi=\Omega t\,. \quad (11)$$

Substituting (11) in (10) we receive:

$$F(\varphi)=F_0+\sum_{k=1}^{\infty}\left(F_k\cos(k\Omega t)+P_k\sin(k\Omega t)\right) \tag{12}$$

(φ = 0…360⁰).

Based on the dependence (2), the modes of the impeller forced vibration are determined, the frequencies of which are critical from the point of view of the rotor entering resonance. For these modes, the values of the exciting force are determined using the dependence (12), and for these modes further analysis is carried out.

For the forced vibration modes that are dangerous from the point of view of the rotor entering resonance, firstly the vibration amplitudes excited by a periodic exciting force, without taking into account damping are determined. The dependences between the amplitudes with and without taking into account damping in the blade crown is determined by the dependence (13):

$$a=\Lambda\bar{a} \tag{13}$$

where a is the amplitude of the impeller forced vibration taking into account damping; Λ is the function that takes into account the effect of damping; $\bar{a}$ is the impeller forced vibration amplitude taking into account damping.

The function Λ is determined by the energy balance method. In this case, it states the fact that the work of the gas-dynamic force during one vibration period is equal to the sum of the work of internal and surface friction:

$$A(\Lambda)=A_{f1}+A_{f2} \tag{14}$$

where $A(\Lambda)$ is the work of gas-dynamic force; A_{f1} is the work of internal friction forces; A_{f2} is the work of surface friction forces.

A similar energy balance must be compiled for each finite element in the contact zone of the blade bandages. The work of internal friction forces for a given finite element is calculated according to the method given in [15] for the case of quasi-viscous friction in an elastic-plastic material:

$$A_{f1}^{e}=\frac{\upsilon-1}{\upsilon+1}\left(\frac{Ea}{2\sigma_m}\right)^{\upsilon+1}\frac{(2\sigma_m)^2}{E} \tag{15}$$

where A_{f1}^{e} is the work of internal friction forces for each finite element; ν is the Poisson's ratio of the blade material; E is the Young's modulus of the blade material; a is the amplitude of forced oscillations of the blade crown; σ_m is the yield strength of the blade material.

The work of internal friction forces for the entire impeller is determined on the base of (15):

$$A_{f1}=\sum_{e=1}^{j}A_{f1}^{e} \tag{16}$$

To determine the work of surface friction for each finite element, we use the following dependence:

$$A_{f2}^{e}=\oint \phi F_C^e X d\delta \tag{17}$$

$$A_{f2}=\sum_{e=1}^{j}A_{f2}^{e}$$

(e = 1…j)

where ϕ is a coefficient of sliding friction for the blade material; F_C^e is a centrifugal force for a given finite element; X is a distance from the rotor axis to the finite element; δ is a generalized displacement of the nodes of the finite element at the contact points of the bandages.

Substituting (15) and (17) into (14), we obtain the amplitudes of the impeller forced vibration taking into account damping by the bandages.

3.3 Solution Adequacy

The accuracy and convergence of the solution should be analysed. To do this, we will consider the influence of several types of finite element meshes, in particular tetrahedral and the hexagonal, on the first most loaded impeller blade free oscillations. The obtained frequencies will be compared with the experimental data given in [12].

Table 1. Influence of the finite elements type on the blade's natural frequency

Oscillation mode	Natural frequency f, Hz		
	Tetrahedron element	Hexagonal element	Experi-ment
m = 0, n =1	1455	1409	1382
m =1, n =1	2031	2014	1984
m = 0, n =2	2580	2547	2530
m = 1, n =2	3009	2972	2956
m = 0, n =3	3685	3658	3631
m = 1, n =3	4190	4160	4146

The data given in Table 1 show that the natural frequencies of the blade, calculated using the hexagonal finite element mesh, have a much smaller discrepancy with the experimental data. Therefore, the developed mathematical model is adequate.

4. Results and Discussion

4.1 Influence of the Boundary Conditions and Bandage Type on the Impeller Frequencies

It should also be noted that the value of the impeller forced vibration frequency is significantly influenced by the type of connection of the blades in the impeller. Herringbone-type shanks connect the blades with the disks, forming a rigid clamping. Bandages connect the blades to each other. Given the presence of mounting tension between the bandages of adjacent blades, it can be assumed that for the impeller forced vibration study, boundary conditions of *C-S* type can be set. That is, rigid clamping (*C*) and elastic connection (*S*).

Based on the damping dependencies given in Subsection 3.2, we consider the influence of the blades bandages design parameters on the impeller forced vibration frequencies. First, we consider the influence of the presence of slippage on the bandages contact zones. The data, presented in Table 2, shows the impeller forced vibration frequencies for two types of boundary conditions of blades bandages contact: *C-C* (rigid clamping on the flanges) and *C-S'* (slippage on the flanges).

Table 2. Influence of boundary conditions on the impeller forced vibration frequency

Harmonic index, k	Forced vibration frequency f, Hz		Discrepancy, %
	C-C	*C-S'*	
1	895.19	868.27	3.1
2	1978.04	1876.70	5.4
3	2235.09	2090.82	6.9
4	3404.01	3175.40	7.2

The data, presented in Table 2, indicate that in the case of slippage presence, the impeller forced vibration frequency decreases. The reason for this is structural damping. The shape of the bandage is designed in such a way as to increase the contact area of adjacent blades bandages and thereby increase the contribution of structural damping in reducing the vibration frequencies. It should be noted that with a change of the vibration mode, the effect of damping also increases, since the discrepancy between the vibration frequencies with and without slippage increases. Thus, for the fourth and third modes (k = 3 and k = 4), which, as was determined above, are close to resonant, the discrepancy is approximately 7%. This is an additional safeguard against the impeller's entering resonance in the case of possible sharp jumps in flow pressure caused by uneven fuel combustion in the GTE combustion chamber, which, in turn, leads to flow pulsations at the inlet to the turbine tract.

Next, the influence of the bandage geometric characteristics that can affect the level of structural damping is considered. Based on the design of the bandage, the most important are its thickness and width.

Table 3. Influence of the bandage width on the impeller forced vibration frequency

Harmonic index, k	Bandage width b, mm		
	5.0	7.5	10.0
	Forced vibration frequency f, Hz		
1	887,14	876,18	868,27
2	1900,03	1891,14	1876,70
3	3041,81	3005,98	2090,82
4	3236,24	3199,41	3175,40

Table 4. Influence of the bandage thickness on the impeller forced vibration frequency

Harmonic index, k	Bandage thickness c, mm		
	2.5	2.65	2.8
	Forced vibration frequency f, Hz		
1	884.14	875.39	868.27
2	1892.03	1889.14	1876.70
3	3008.81	3001.98	2090.82
4	3194.24	3187.41	3175.40

Analysis of the data given in Tables 3 and 4 allows us to assess the influence of structural damping on the impeller forced vibration frequencies. It is clear that the influence of the width of the bandages is more significant, because it depends on the value of such a parameter as the slip length. So, from Table 3 it can be seen that for the fourth vibration (k = 4) the difference between the forced vibration frequencies for the largest and smallest widths, due to the design of the side surfaces of the bandage, is 61 Hz. But, on the other hand, a significant increase in the width of the bandage leads to an increase in the mounting tension during the technological operations of impeller assembling and, as a result, increases its rigidity.

The data from Table 4 also allow us to assess the influence of the thickness of the bandage on the impeller forced vibration frequencies. We also see that increasing of the bandage thickness leads to a decrease in the impeller forced vibration frequency although this effect is not as significant as for the bandage width. For the most dangerous fourth mode, the difference between the forced vibration frequencies corresponding to the largest and smallest thicknesses is only 18 Hz. With an increase of the bandage thickness the vibration frequency decreases, but a significant increase in the thickness of the bandage also leads to a significant increase in its stiffness and, as a result, the impeller forced vibration frequency also increases.

Taking into account that the studies were conducted concerning the parameters of the working fluid flow, which corresponds to the steady-state operating mode of the engine, we can conclude that the parameters given in Table 3 and Table 4 are the most optimal in terms of using the advantages of structural damping for this type of GTE.

In gas turbine engineering practice, two types of blade bands are used: arched and *Z*-shaped. The data, given in Table 5, shows the influence of the bandage type on the impeller forced vibration frequencies.

Table 5. Influence of bandage type on the impeller forced vibration frequency

Bandage type	Harmonic index, *k*	Forced vibration frequency *f*, Hz
Z-shaped	1	868.27
	2	1876.05
	3	2090.80
	4	3175.40
Arc bandage	1	998.51
	2	2157.46
	3	2278.97
	4	3413.55

The data given in Table 5 show that the natural frequencies of the blade, calculated using the hexagonal finite element mesh, have a much smaller discrepancy with the experimental data. Therefore, in the future, for mechanical calculations, this type of finite elements will be used.

4.2 Amplitude-Frequency Characteristics of the Impeller

In order to study the practical suitability of the developed mathematical model, calculations of the second stage gas turbine impeller forced vibration amplitudes and frequencies are calculated. As it is well-known, for the marine gas turbine engines there are two main constructional types of the impellers: an impeller with a disk having a central shaft hole and with a solid disk. The heterogeneity of the gas flow, which is the main source of the impeller forced vibration, was set by the deviation of the nozzle vanes installation angle from its nominal value. Also the unevenness of the twist angle along the blades height was taken into consideration. In addition, damping was taken into account at the points of contact between the blades, the blades and the disk and the blades and damper links.

The studied impeller consists of 65 working blades of variable cross section with damping links. The height of the blade is l = 115 mm; the material of the blades is a heat-resistant alloy (material density is ρ = 8100 kg / m^3, Young's modulus is E = 1.79x10^6 MPa, Poisson's ratio is υ = 0.3). The diameter of the disk is D = 375 mm. The exit angle of flow from the nozzle channels α_1 was changed from $16^\circ30'$ to $18^\circ30'$; the exit angle of flow from the impeller is $\alpha_2 = 73^\circ$.

The information on Figure 2 shows the amplitude-frequency characteristic of the marine gas turbine second stage impeller forced vibration, caused by the non-stationary gas flow of the fourth harmonic (k = 4). The resonance frequency of the impeller ω_p = 1325 Hz.

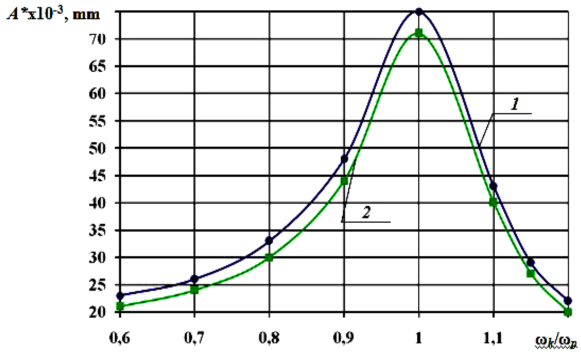

Figure 2: Amplitude-frequency characteristic of the impeller forced vibration:
1 – impeller with a disk having a central shaft hole;
2 – impeller with a solid disk

Analysing graphical dependencies presented in Figure 2, it can be concluded that the amplitude of the impeller forced vibration increases smoothly when approaching the resonant frequency of vibration for types of the impeller construction. Then, when the resonance frequency is reached, there is a sharp increase, and after passing through the resonance state, there is a sharp drop and then a gradual decrease in the amplitude. As it is known, the resonance occurs when the frequency of the impeller forced vibration coincides with the frequency of turbine rotor rotation. Therefore, the knowledge of the forced vibration frequencies allows to carry out the so-called detuning from the resonant mode. It is sufficient to exclude the occurrence of resonance in the range of operating frequencies, translating it into fast-running modes of the engine starting and stopping. You can also avoid preventing the coincidence of the turbine rotor rotation frequency with the impeller frequency of forced vibration by changing the parameters of the gas flow, especially, reducing the gas pressure drop before and after the considered turbine stage. This will give an opportunity to reduce the variable component of the gas-dynamic force, which arises due to the turbulence of the gas flow and is the main cause of the impeller vibration. Another way to improve the instability of gas flow is to reduce the structural heterogeneity of the nozzle array that means to reduce the deviation of the nozzle vanes installation angle from the nominal value.

Another important conclusion which can be made analysing Figure 2, is that at the same frequencies, the vibration amplitudes of the impeller with a solid disc (curve *2*) are lower than those of the impeller having a disc with a central shaft hole (curve *1*). It can be explained by the fact that an impeller with a solid disc is more rigid.

4.3 Forced Vibration Frequencies and Modes of the Impeller

The next stage of the analysis involves the consideration of the impeller's forced vibration modes and frequencies. All frequency values have been determined for the first three vibration modes.

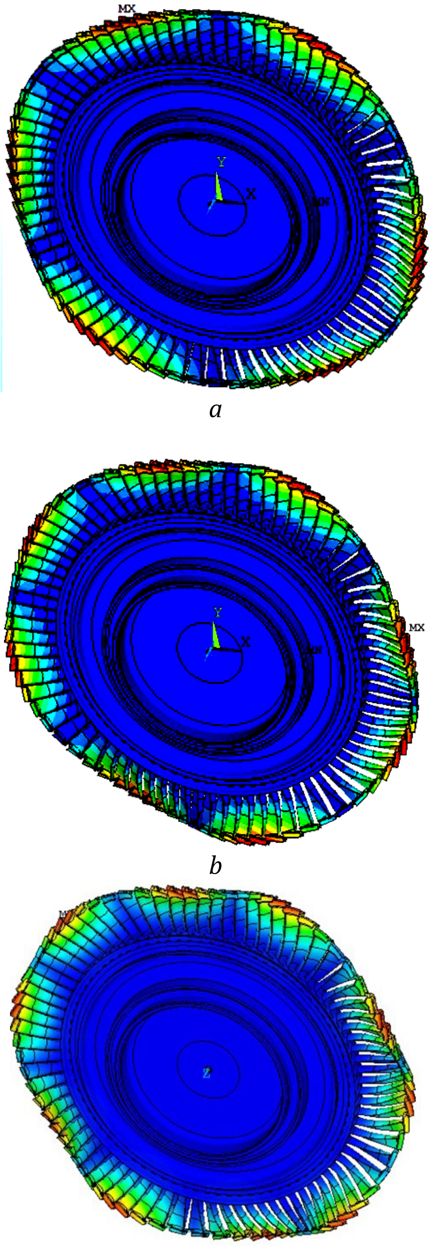

a

b

c

Figure 3: The impeller forced vibration modes:
a – *k* =3, *f* = 886 Hz; *b* – *k* =4, *f* = 909.7 Hz;
c – *k* =5, *f* = 970.5 Hz

Analysis of the data represented on the Figure 3 shows that increasing of the vibration mode, the impeller forced vibration frequency also increases. The increase of the forced vibration frequency is also associated with an increase in number of the impeller nodal diameters, which, in turn, leads to the presence of more complex deformations of the impeller.

Also, it could be found out that for all given types of impeller modes they change from the bending mode at the peripheral area to the torsion mode near the nodal diameters. It should be also mentioned that for the impeller with less quantity of nodal diameters they are more obvious and its amplitude is much slider. The explanation of this fact is its higher ductility.

5. Conclusions

The article presents the main provisions of the improved mathematical model of a compact single-shaft gas turbine engine rotor impellers forced vibration. It takes into account the complex influence of pressure and high temperature of the turbulent working fluid flow of on the impeller forced vibration frequencies. The influence of centrifugal force is also taken into account. The proposed mathematical model differs from the existing ones by the complex consideration of the simultaneous influence of all factors that cause the impeller forced vibration during its operation process.

A detailed study of structural damping influence on the impeller forced vibration frequencies is also held. The advantages of the proposed model include its versatility, which allows it to be used for the analysis of turbine rotor impellers of any gas turbine engine regardless of the number of impellers in the rotor assembly and the geometric characteristics of the blades and disks. The isoparametric eight-node curvilinear finite elements used in the development of the refined mathematical model give an opportunity for high-precision study of both uncooled blades and disks and structurally inhomogeneous cooled blades. Moreover, the shape of the finite elements for approximating the solid-state rotor model is as close as possible to the shape of finite volumes, which were used in computational flow dynamic analysis. That minimises the calculation error.

Considerable attention was paid to the issue of more accurate determination of the impeller forced vibration frequencies. It was investigated which vibration frequencies and for which modes are critical from the point of view of the impeller entering resonance state. The amplitudes of the impeller forced vibration were determined for each of the studied modes. In addition, the dependence of the amplitudes of impeller forced vibration on the pressure drop of the gas flow passing through the impeller was obtained.

The influence of structural damping on the forced vibration frequencies of the impeller was also investigated in detail. When conducting research, it was assumed that "springs" were installed in the contact points of the bandages. Depending on the "spring stiffness", which corresponds to the installation tension, two types of boundary conditions between the bandages were set: rigid clamping and slipping, and the impeller forced vibration frequencies were also determined. For each forced vibration mode, a study was conducted, that pays attention to the influence of the geometric parameters of the blade bandages on the impeller forced vibration frequencies.

The optimal thicknesses of the blade's bandages for the GTE of this type were established from the point of view of vibration damping. A comparative analysis of the influence of the blades bandages design on the impeller forced vibration frequencies. The arched and *Z*-shaped bandages, which are the most common in gas turbine practice, were taken into consideration. It was found that the use of *Z*-shaped bandages is more appropriate for increasing the structural damping effect.

References

[1] Dobridenko, O., Voitenko, S., Tereshchenko, Y., Yakovlieva, A., Boshkov, V., & Trofimov, I. (2024). Statistical analysis of aircraft gas turbine engine failures caused by quality of fuel. *2024 New Trends in Aviation Development (NTAD), Stary Smokovec, Slovakia.* 26-31. https://doi.org/10.1109/NTAD63796.2024.10850293

[2] Shakurova, L., Armenise, I., Kustova, E. (2023). Effect of slip boundary conditions on nonequilibrium reacting air flows. *Journal of Theoretical and Applied Mechanics,* 53(3), 253–269. https://doi.org/10.55787/jtams.23.53.3.253

[3] Arnab, B., Prabhakar, S., Giacomo, C. (2023). Natural frequency analysis of a functionally graded rotor-bearing system with a slant crack, subjected to thermal gradients. *International Journal of Turbo and Jet Engines,* 40(3), 243 – 255. https://doi.org/10.1515/tjj-2021-0002

[4] Chenglong, Sh., Yanhong M., Yongfeng, W., Xueqi, Ch., & Jie, H. (2025). Influence of conical shaft stiffness on the dynamic characteristics of flexible rotor. *International Journal of Turbo and Jet Engines*, 42(1), 102-116. https://doi.org/10.1515/tjj-2024-0073

[5] Valeev, S., Kondratyeva, N. (2022). Life test optimization for gas turbine engine based on life cycle information support and modeling. *Energies,* 15, 68 – 74. https://doi.org/10.3390/en15196874

[6] Yuan, J., Gastaldi, Ch., Goy, E.D., & Chouvion, B. (2024). Friction damping for turbomachinery: a comprehensive review of modeling, design strategies and testing capabilities. *Progress in Aerospace Science*, 147. https://doi.org/10.1016/j.paerosci.2024.101018

[7] Yershov, S.V., Yakovlev, V.A. (2021) The influence of mesh resolution on 3D RANS flow simulations in turbomachinery flow path. *Journal of Mechanical Engineering*, 24(1), 13–27. https://doi.org/10.15407/pmach2021.01.013

[8] Wang, S., Shouzuo, L., Lei, L., Zhao, Zh., Wei, D., & Bengt, S. (2021). A high temperature turbine blade heat transfer multilevel design platform. *Numerical Heat Transfer, Part A: Applications*. 79(2), 122–145. https://doi.org/10.1080/10407782.2020.1835104

[9] Skamniottis, Ch., Courtis, M., Cocks, C. F. (2021). A. Multiscale analysis of thermo-mechanical stresses in double wall transpiration cooling systems for gas turbine blades. *International Journal of Mechanical Sciences*, 58, 49-54. https://doi.org/10.1016/j.ijmec.sci.2021.106657

[10] Seok, S., Shahriar, A., Montoya, A. (2023). A finite element approach for simplified 2D nonlinear dynamic contact impact analysis. *Archieves of Applied Mechanics*. 93, 3511 – 3531. https://doi.org/10.1007/s00419-023-02451-y

[11] Duriagina, Z. A., Kulyk, V. V., Filimonov, O. S., Trostianchyn, A. M., & Sokulska, N.B. (2021). The role of stress-strain state of gas turbine engine metal parts in predicting their safe life. *Progress in Physics of Metals*, 22(4), 643–677. https://doi.org/10.15407/ufm.22.04.643

[12] Smetankina, N., Morhun, S. (2025). Determination of the stress-strain state of the rotor of an improved single shaft gas turbine engine. *Strength of Materials*, 57(1), 58-68. https://doi.org/10.1007/s11223-025-00746-9

[13] Yalin, Sh., Lingling, Ch., Pengfei, Ch., Qingzhen, Ya., Yongqiang, Sh., & Hua, Ya. (2024). Numerical study on aerodynamic performance of an intake duct affected by ground effect. *International Journal of Turbo and Jet-Engines*, 41(4), 803-814. https://doi.org/10.1515/tjj-2022-0056

[14] Smetankina, N., Morhun, S. (2024). The modern single shaft gas turbine rotor stress-strain state determination taking into account the contact thermoelasticity problem. *Technicki vjesnik*, 31(2), 551-556. https://doi.org/10.17559/TV-20230628000770

[15] Almarahlleh, N. H., Al-Suod, M. M. S., Morhun, S., Smetankina, N., & Zhuk, I. (2026). Determination of the modern marine gas turbine rotor forced vibration parameters by numerical and experimental methods. International Journal of *Electrical and Electronic Engineering and Telecommunications*, 15(1), 63-71. https://doi.org/10.18178/ijeetc.15.1.63-71